metals

MDPI

Article

Study of Mineralogy and Metallurgical Properties of Lump Ores

Deqing Zhu, Yin Jiang *, Jian Pan and Congcong Yang

School of Minerals Processing and Bioengineering, Central South University, Changsha 410083, China
* Correspondence: 205611061@csu.edu.cn

Abstract: The ironmaking process in blast furnaces using iron lumps is an energy-efficient and low-carbon initiative that helps lower the cost of the ironmaking process. The physical and chemical properties of raw materials, process mineralogy, and metallurgical properties of three Malaysian iron ore lumps were researched in this paper, with the goal of showing the relationship between metallurgical qualities and mineralogy. The results show that lump ore A has a better decrepitation index, with a $DI_{-6.3mm}$ of only 0.2%; lump ore J has better reducibility and low-temperature reduction disintegration index, with RI and $RDI_{+6.3mm}$ values of 88.39% and 87.55%, respectively; and the three lump ores have excellent softening and melting properties and a high permeability index. The metallurgical properties of lump ore and mineralogical characterizations are generally correlated, the decrepitation performance of lump ore is mostly determined by the presence of goethite, and the original porosity is unrelated. The higher the content, the worse the decrepitation performance; lump ore's reducibility is mostly determined by the open porosity and the content of newly generating hematite at high temperatures, which has no relationship to its original porosity. The higher the open porosity, the higher the goethite content, the higher the newly generated porous hematite content, and the better the lump ore's reducibility; the higher the original hematite content in the lump ores, the lower the open porosity at high temperatures and the worse the reduction degradation characteristics.

Keywords: ore iron lump; mineralogy; open porosity; goethite; metallurgical properties

Citation: Zhu, D.; Jiang, Y.; Pan, J.; Yang, C. Study of Mineralogy and Metallurgical Properties of Lump Ores. *Metals* **2022**, *12*, 1805. https://doi.org/10.3390/met12111805

Academic Editor: Andrii Kostryzhev

Received: 17 August 2022
Accepted: 18 October 2022
Published: 25 October 2022

1. Introduction

With the rapid development and innovation of the Chinese steel industry over the past decades, the mixed burden structure of the domestic blast furnace ironmaking process primarily utilizes the dosage mode of "high basicity sinter + acid pellet + iron lump ore," with sinter and pellet accounting for more than 80% of the BF [1–5]. However, the production of sinter and pellet ore inevitably results in a number of challenging environmental issues such as excessive energy consumption, hazardous flue gas emissions, and noise pollution. In light of the "carbon peaking and carbon neutrality goals," the requirement for energy savings and emission reductions in the ironmaking process is becoming increasingly important [6–12]. As a result, it is critical to conduct a systematic study on iron lump ores to minimize production costs, to reduce pollution, and to increase economic and social profits.

The lump ore ratio has a significant influence on the metallurgical properties of the burden and the BF operation. In recent years, a large number of researchers have studied the metallurgical characteristics of various lump ores and the smelting behavior in the blast furnace to reduce production costs and increase economic and social benefits [13–17] In addition, the metallurgical properties of lump ore are key factors in the overall blast furnace ironmaking process and the quality of the product, while the metallurgical properties of lump ore are influenced to some extent by its physicochemical properties and

structure [18–23]. For example, Bristow et al. [21] found that the structure of the raw materials before the reduction was characterized and found to be correlated with the reducibility, and a higher volume of pores less than about 10 μm in diameter had a positive impact on the reducibility of the sample. Harvey [22] also revealed that the chemistry of ore and the heating conditions may be the central influencing factors on the formation of melt, porosity, and mineralogy, and pore distribution and total porosity of the sinter were found to be well-linked with compressive strength and reducibility. In addition, some researchers have deemed that the softening and melting (S & M) behavior of iron lump ore in a blast furnace may be optimized by complex chemical and physical interactions between sinter and lump at high temperatures. However, predecessors have not conducted a comprehensive study on the relationship between the nature of the lump ore and its metallurgical properties at high temperatures.

Therefore, to address the gap in research, in this article, we examine the physical and chemical properties of raw materials, process mineralogy, and metallurgical properties of three imported lump ores from Malaysia, and reveal the relationship between their process mineralogy and metallurgical properties to provide a guideline for BF operation to improve the proportion of lump ore and to optimize the process parameters.

2. Experimental Section

2.1. Materials

Malaysia produces three natural iron lump ores: AC (also referred to simply as lump ore A), JLD (also referred to as lump ore J), and SEB (also referred to as lump ore S). The chemical compositions of the three lump ores are shown in Table 1. Among the three types of lump ores, lump ore A had the largest TFe content (61.45 wt%), followed by lump ore S with 60.01 wt%, and lump ore J had the lowest TFe content (55.08 wt%), which is mostly correlated to the water for crystallization and lode mineral content. Furthermore, the value of the loss on ignition (LOI) and SiO_2 content of lump ore A were the lowest, at 4.93 wt% and 3.35 wt%, respectively, whereas lump ore J had the highest, at 10.64 wt% and 8.03 wt%, respectively.

Table 1. Chemical compositions of three iron lump ores.

Type	TFe	FeO	SiO_2	CaO	MgO	Al_2O_3	K_2O	Na_2O	P	S	Pb	Zn	LOI
A	61.45	4.45	3.35	0.09	0.10	2.91	0.03	0.022	0.039	0.097	0.12	0.073	4.93
J	55.08	0.54	8.03	0.34	0.16	1.05	0.16	0.036	0.046	0.021	0.018	0.055	10.64
S	60.01	3.23	2.60	1.54	0.34	1.84	0.014	0.012	0.080	0.034	0.026	0.085	6.80

The physical properties of the three lump ores are shown in Table 2. The open porosity of lump ore S was the largest, reaching 16.54%; the open porosity of lump ore J was the lowest, at 4.23%; and the open porosity of lump ore A was between the two, at 12.08%. The open porosity of the lump ores affects reducibility to some extent, and generally speaking, lump ores with high porosity have superior reducibility. However, because all iron ores contain varying amounts of water for crystallization and carbonate minerals, a large number of pores and cracks may form under high-temperature conditions, and the final reducibility of the lump ore will be largely determined by the actual open porosity under high-temperature conditions. In terms of particle size composition, the +10 mm particle size grades of the three lump ores were above 90%, while the content below −5 mm was less than 5%, which could meet blast furnace production requirements.

Table 2. Physical properties of three types of natural lump ores.

Type	Bulk Density/g/cm³	Apparent Density/g/cm³	Open Porosity/%	Particle-Size Distribution/(mm)%						
				+40	40–25	25–16	16–10	10–6.3	6.3–5	–5
A	3.50	3.98	12.08	6.89	15.84	21.79	48.45	4.6	0.07	2.36

J	3.63	3.79	4.23	11.03	20.95	19.89	41.34	0.05	4.53	2.2
S	2.78	3.33	16.54	13.38	17.95	21.19	38.67	4.62	0.05	4.15

2.2. Methods

(1) Characters of lump ores

Several sets of parallel samples were generated by shrinkage sampling according to GB/T103221-2000 after mixing the three types of lump ores, which mostly eliminated the interference of accidental factors. The chemical composition was determined by chemical titration method. The determination of bulk density and apparent density of lump ore is based on Archimedes' principle, and the specific determination method refers to the Chinese standard GB-24240-2009; the calculation method of open porosity is $\rho = 1 - \rho_1/\rho_2$ (ρ_1, bulk density; ρ_2, apparent density). The conditions of XRD(D/MAX2500X diffractometer) are Cu target, tube voltage 40 kV, tube current 30 mA, diffraction angle 5°~80°, and scanning speed 4°/min.

(2) Mineralogy

First, 20~30 representative samples with particle sizes ranging from 3 to 5 mm were obtained through crushing, mixing, and shrinkage sampling, and were mounted and polished using a semi-automatic grinding and polishing machine (Tegramin-25, Danish Struers Company, Copenhagen, Denmark) to produce light flakes for mineral phase analysis. The microstructure was identified using an optical microscope (model LeicaDM4500P, Leica, Germany), and the percent content of the main mineral phases was calculated using area statistics, with a minimum of 50 statistical areas. The distribution characteristics and content of Fe, Al, Si, and other elements were characterized using SEM and EDS (SEM, MIRA4 LMH; EDS, One Max 50).

(3) Metallurgical properties

The metallurgical properties of the three lump ores were determined, including the decrepitation performance (DI), reducibility (RI), low temperature reduction degradation index (RDI), and softening and melting performance (S & M), to comprehensively evaluate and predict the smelting behavior of different lump ores in the blast furnace. The DI, RI, RDI, and (S & M) of the lump ores were measured and evaluated under Chinese standards GB/T10322.6-2004, GB/T13241-1991, GB/T13242-2017, and GB/T34211-2017, respectively. For the softening and melting performance (S & M), T_a, T_s, T_m, and T_d represent starting softening temperature, softening termination temperature, starting melting temperature, and starting softening temperature, respectively.

3. Results and Discussion

3.1. Mineralogy

3.1.1. Phase Analysis

The XRD analysis findings of three natural lump ores (A, J, and S) from Malaysia are shown in Figure 1 for the qualitative mineral composition analysis. The analysis revealed that the main mineral phases of lump ore A were hematite, goethite, magnetite, and quartz, but no apparent aluminous minerals were found; goethite and quartz were the main mineral phases of lump ore J; and goethite, hematite, magnetite, and a little quartz were the main mineral phases of lump ore S. When lump ore A and S are compared, the key difference is that lump ore A has a larger proportion of magnetite and quartz, whereas lump ore S has a smaller content of goethite.

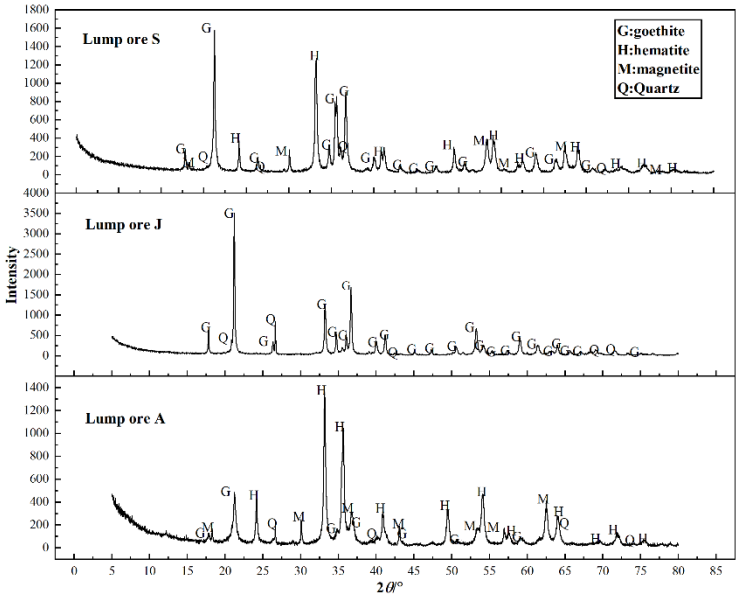

Figure 1. XRD analysis results of the three lump ores.

3.1.2. Microstructures

The microstructures of the three types of the Malaysian lump ores are closely related to their physicochemical properties, as shown in Figures 2 and 3 (H is hematite, M is magnetite, G is goethite, Q is quartz, K is kaolinite, P is pore), and the mineral composition contents of the three types of lump ores are shown in Table 3.

Table 3. The main mineral composition of the three lump ores.

Type \ Content/wt%	Hematite/%	Magnetite/%	Goethite/%	Quartz/%	Kaolinite/%	Other/%
A	42.56	14.19	35.03	5.84	/	2.38
J	/	/	90.40	5.94	2.24	1.42
S	26.74	9.64	55.83	3.02	3.12	1.65

(1) Lump ore A

From Table 4, it can be observed that hematite, magnetite, goethite, and quartz were the main minerals in lump A. It can be seen that the hematite content was 42.56 wt% in Table 3, primarily in the form of grains, with grain sizes ranging from tens to hundreds of microns. Figure 2 a~f shows the microstructure and main physical phases of lump A. It can also be observed that the surfaces of magnetite grains were slowly oxidized to generate pseudo-hematite, which was frequently coeval with minerals such as goethite and magnetite. Additionally, the content of goethite was 35.03 wt%, as summarized in in Table 3, which was mostly filled between the grains of hematite and magnetite in the form of dissemination; magnetite was 14.19 wt%, which frequently formed coarse aggregates with well-developed grains, mainly semi-automorphic and automorphic crystals; and quartz was mostly seen embedded in goethite with microfine grains.

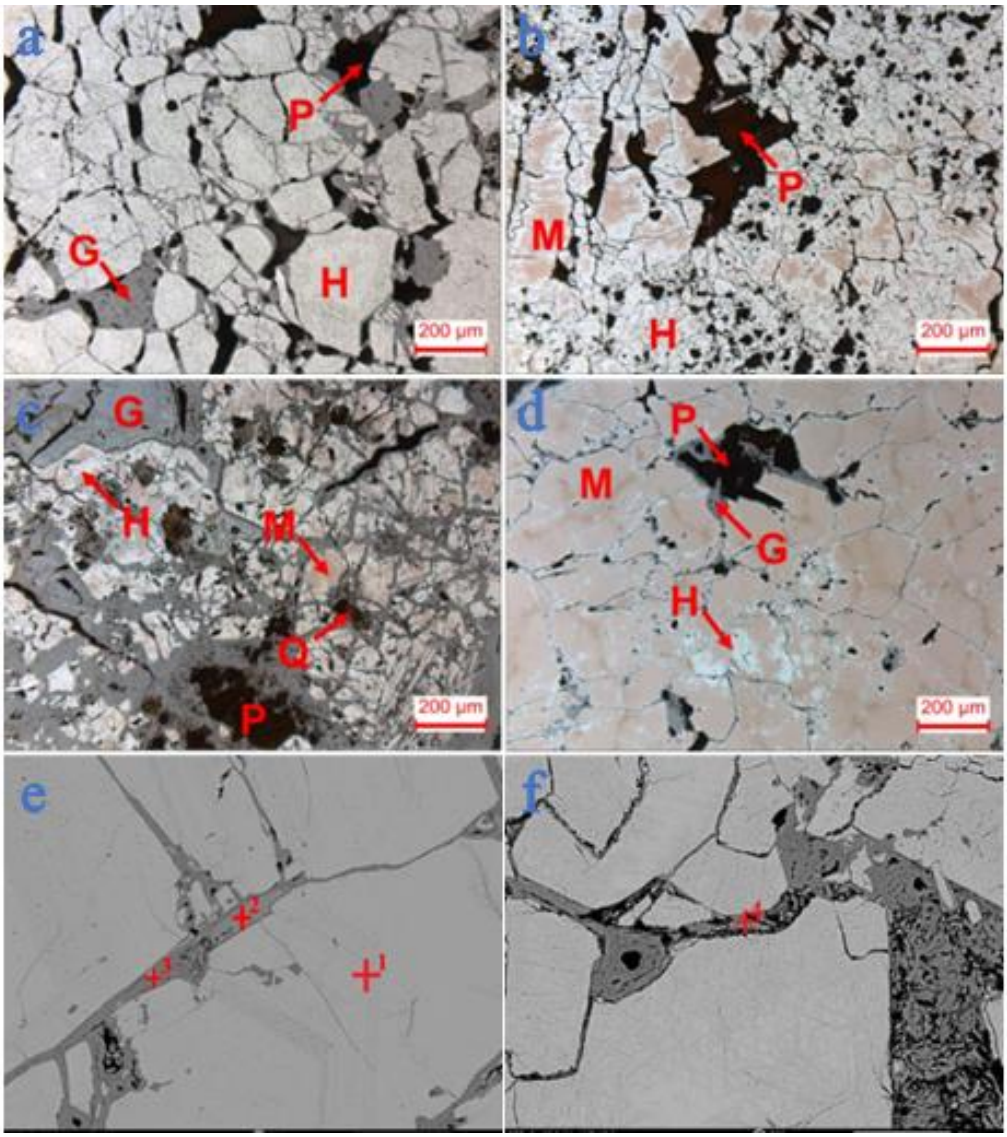

Figure 2. Microstructure and main physical phases of lump A. (**a**-**f**)

Table 4. EDS analysis results for areas in Figure 2.

Area	Atomic/%				Mineral Constituent
	O	Al	Si	Fe	
1	55.30	/	/	34.70	Hematite
2	56.64	/	/	42.08	Magnetite
3	74.98	0.89	0.48	23.65	Goethite
4	71.70	/	28.30	/	Quartz

(2) Lump ore J

As shown in Table 5, the mineral composition of lump ore J was simpler than that of lump ore A, consisting primarily of goethite and quartz, with a trace of kaolinite and quartz. The goethite content was 90.40 wt%, as listed in Table 3, and the structure was more compact; the quartz and kaolinite contents were 5.94 wt% and 2.24 wt%, respectively, as listed inTable 3, whose particle sizes ranged from microns to several hundred microns, and they were mainly embedded in goethite minerals as rods and grains, as shown in Figure 3 a–e.

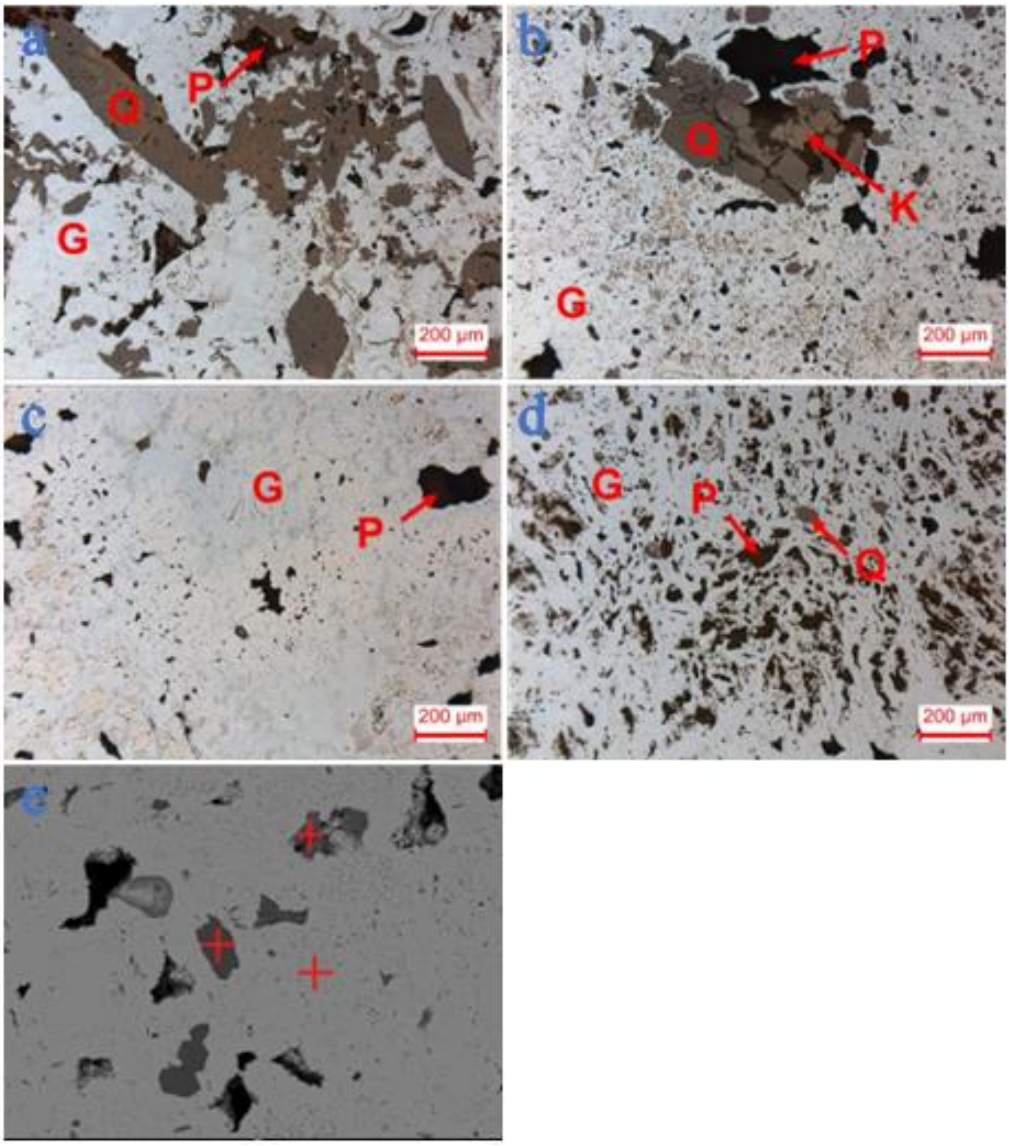

Figure 3. Microstructure and main physical phases of lump J. (**a-e**)

Table 5. EDS analysis results for areas in Figure 3.

Area	Atomic/%						Mineral Constituent
	O	Al	Si	Fe	Mg	K	
1	66.08	13.63	14.85	0.82	0.5	0.09	Kaolinite
2	71.43	/	28.57	/	/	/	Quartz
3	74.98	/	0.94	24.08	/	/	Goethite

(3) Lump ore S

As shown in Table 6, the major mineral component of lump ore S was identical to that of lump ore A. The goethite content reached 55.83 wt%, as listed in Table 3, some aluminum and silicon elements were intermingled, and the majority of the goethite structure was loose and porous, as shown in Figure 4A-G. Hematite had a content of 26.74 wt%, as listed in Table 3, and two types of morphology: one was irregularly generated by goethite dehydration, and the other was a granular structure with semi-automorphic crystal output. Figure 4a-g shows the microstructure and main physical phases of lump S. Magnetite had a weight percentage of 9.64 wt%, as listed in Table 3, and was usually found in close association with hematite and goethite, which was created by goethite dehydration.

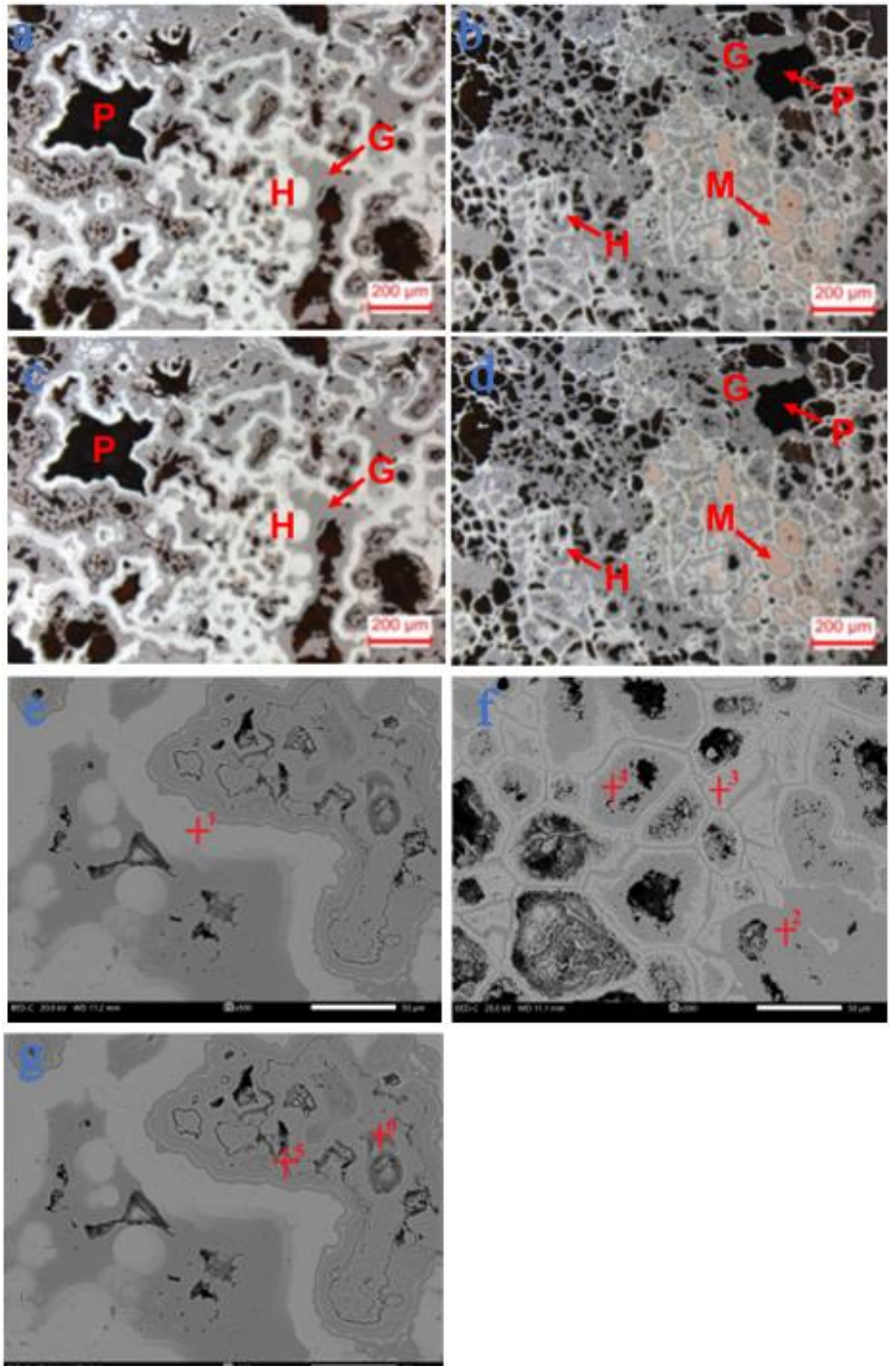

Figure 4. Microstructure and main physical phases of lump S. (**a**-**g**)

Table 6. EDS analysis results for areas in Figure 4.

Area	Atomic/%					Mineral Constituent
	O	Al	Si	Fe	Mg	
1	78.09	3.30	0.90	17.71	/	Alum goethite
2	68.21	/	/	31.57	/	Goethite

3	58.21	0.30	0.67	40.52	/	Hematite
4	56.20	/	/	43.23		Magnetite
5	71.53	8.54	7.41	10.55	1.97	Kaolinite

3.2. Metallurgical Property

To assess the overall quality of the three Malaysian lump ores, metallurgical properties tests were determined, and the relationship between their metallurgical properties and mineralogical characterizations was examined.

3.2.1. Decrepitation Performance

Figure 5 depicts a comparison of the decrepitation performance of the three types of lump ore. As shown in the Figure 5, lump ore A had the best decrepitation performance, i.e., $DI_{-6.3mm}$ was just 0.2%, followed by lump ore S ($DI_{-6.3mm}$ was 1.9%), and lump ore J had the worst decrepitation performance ($DI_{-6.3mm}$ was 5.8%). According to Figure 6, the decrepitation performance of lump ore and its LOI (containing crystalline water, goethite mineral, etc.) are highly connected. The higher the goethite concentration in lump ore, the higher the LOI value, the poorer the decrepitation performance of lump ore, and the more powder generated in the upper section of the BF.

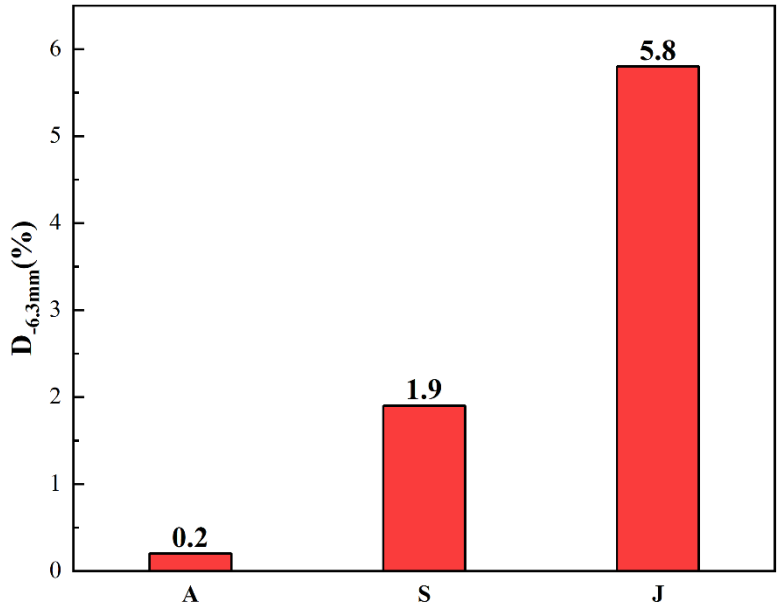

Figure 5. Decrepitation index of three types of lump ores.

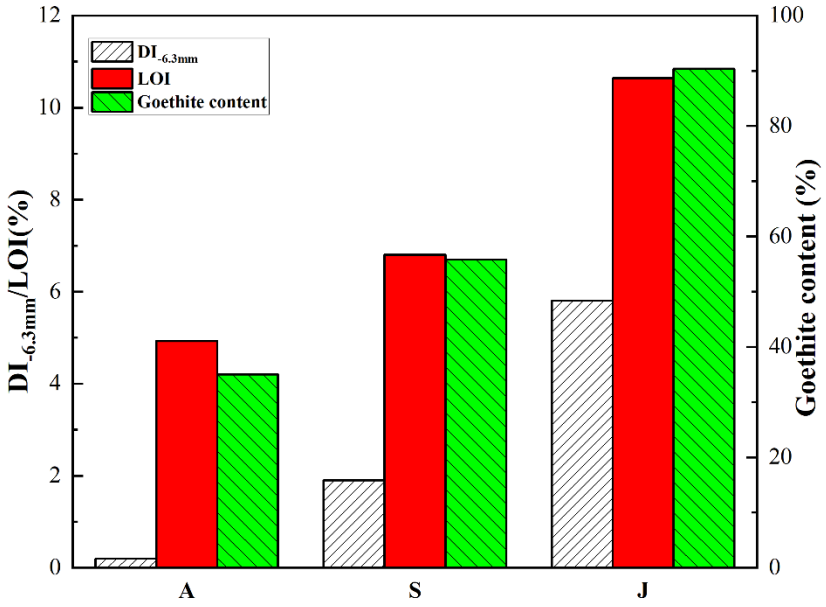

Figure 6. Relationship between fire waste and goethite content and decrepitation performance.

3.2.2. Reducibility Index and Reduction Degradation Index

Because good reducibility of lump ore is conducive to an indirect reduction reaction in the BF, lowering coke consumption, and low-temperature reduction disintegration performance is related to the strength of the reduced iron ores. The reducibility and low-temperature reduction disintegration index of the three lump ores are presented in Table 7.

Table 7. Reducibility and low-temperature reduction disintegration index of three lump ores.

Type	RI/%	RDI/%	
		$RDI_{+6.3mm}$	$RDI_{+3.15mm}$
A	71.01	60.42	70.86
J	88.39	87.55	91.74
S	74.50	78.75	84.44

In terms of reducibility, the three lump ores were excellent, with RI over 70%. Lump ore J had the greatest reducibility, followed by lump ore S, while lump ore A was somewhat poorer than lump ore S. The reason for this is that the reducibility of lump ores is connected not only to their original properties but also to their microstructural alterations under high temperature reduction conditions. Therefore, after cooling at 900 °C and under N_2 atmosphere for 1 h, the microstructures of the three lump ores were studied under scanning electron microscopy, and the open porosity was measured.

According to Figure 7, the higher the goethite content of the lump ores, the higher the open porosity at high temperatures, and the better its reducibility. J > A > S was the order of reducibility of lump ores from high to low, as shown in Table 7. The open porosity of lump ores at high temperatures was shown to be strongly connected with their reducibility. This is because the main factors determining the reducibility are the reducibility of the minerals included in the lump ores themselves and the porosity at high temperatures, whereas it has little relationship with its initial open porosity. At an atmosphere of high temperature, the goethite included in the three lump ores thermally decomposed to generate hematite with a loose and porous surface, and its reducibility was better than that of the hematite with the compact original structure. Furthermore, removing the crystalline water in the goethite improves the open porosity of the lump ores, which improves reducibility. Because the lump ores J and S were limonite-type iron lump ores with 90.01%

and 55.01% goethite, respectively, higher goethite concentration means improved reducibility. As seen in Figure 7, the open porosity of lump ores at high temperatures was J > A > S in the order of high to low, which was consistent with their reducibility.

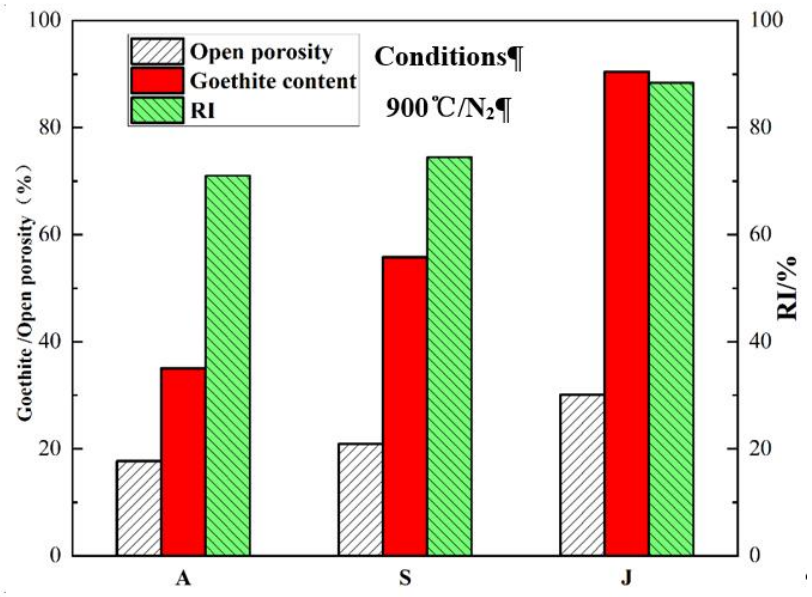

Figure 7. Relationship between the open porosity and the goethite content and the reducibility at high temperatures.

According to Table 7, lump ore J demonstrated the highest anti-disintegration performance among the three lump ores in terms of low-temperature reduction disintegration index, with $RDI_{+3.15mm}$ reaching 91.74% and $RDI_{+6.3mm}$ reaching 87.55%. In general, the higher the content of original hematite in the lump ore, the greater the degree of low-temperature reduction disintegration, but a large number of pores formed by the dehydration of the higher content of goethite in lump ore J and S, to a degree, mitigated the negative effect of volume stress caused by the volume expansion of hematite reduced to magnetite. The degree of low-temperature reduction disintegration is inversely proportional to the open porosity at high temperatures. As a result, the higher the goethite concentration, the higher the open porosity at high temperatures, and the less powder generated by the lump ore in the reduction process. As a consequence, lump ore J reduced well and also resisted low-temperature reduction disintegration.

3.2.3. Softening and Melting Properties

The width and location of the cohesive zone within the blast furnace promote stable blast furnace production operations and better gas consumption. As a consequence, the high temperature softening and melting properties of three types of lump ore are compared, as illustrated in Figure 8.

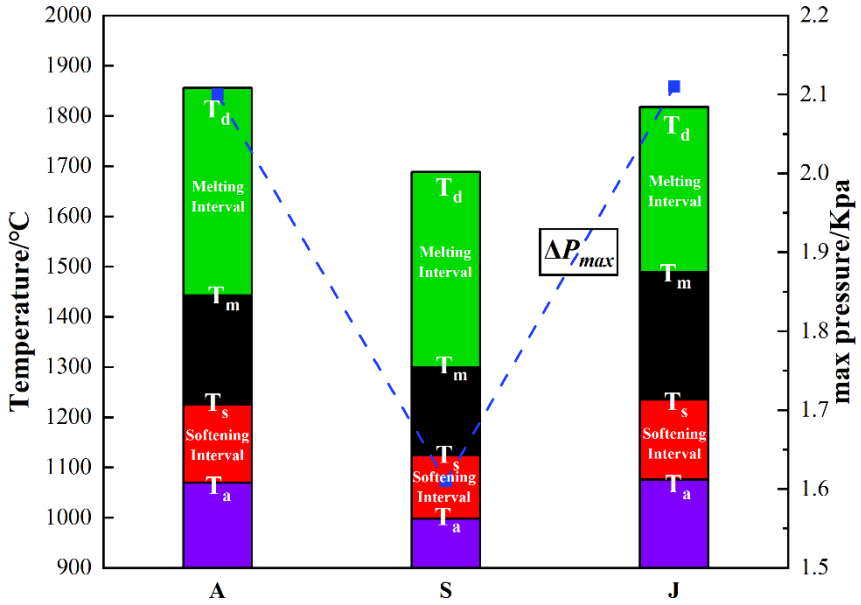

Figure 8. The high temperature softening and melting properties of three lump ores. (T_a, starting softening temperature; T_s, softening termination temperature ; T_m, starting melting temperature; Td, starting dropping temperature; $_{max}$, permeability).

The softening and melting performance of lump ores J and S was superior to that of lump ore A. Furthermore, the softening and melting temperature interval range of lump ore A was 413 °C. The starting dropping temperature was 1483 °C, whereas the starting softening temperature was 1070 °C. This might be due to its increased Al_2O_3 content, which generates a high melting point when the Al_2O_3 level is higher and causes the slag's dropping temperature to rise. Lump ore S had a starting dropping temperature of 1387 °C, which might be attributed to its higher natural basicity, which would be adverse to the softening-melting properties of lump ore. In comparison, lump ore J exhibited the narrowest melting and softening temperature intervals, as well as a respectable dropping temperature. Among the three lump ores, lump ore S exhibited the best permeability and the lowest maximum pressure difference, i.e., ΔP of just 1.61 kPa.

According to the Standard Code for the design of a blast furnace ironmaking plant in China (GB50427-2008), the high-temperature metallurgical properties of three Malaysian lump ores are in accordance with the ironmaking industry standard. Therefore, an interactive test can be conducted to explore the reasonable proportion of furnace charge, and therefore, to optimize the structure of blast furnace charge.

4. Conclusions

(1) Among the three types of lump ores, lump ore A had the best decrepitation performance with a $D_{-6.3mm}$ of 0.2%; lump ore J had the highest reducibility with an RI of 88.39%; lump ore J had the best low-temperature disintegration performance with an $RDI_{+3.15\ mm}$ of 91.74%; and in terms of softening performance, the three types of lump ores had higher starting softening temperature and dropping temperature, and a narrower softening temperature interval. All in all, the comprehensive quality of the three lump ores meets industry standards.

(2) The metallurgical characteristics of the three types of lump ore are strongly connected to their process mineralogy. The decrepitation performance of lump ore is closely related to its process mineralogy; the decrepitation performance and its goethite content (loss on ignition) are closely and positively correlated, with the higher the content, the worse the decrepitation performance; the reducibility of lump ore depends primarily on the open porosity and hematite content and type at high temperatures, with the original open porosity being unimportant. The higher the goethite

content, the larger the open porosity at high temperatures, the more freshly formed porous hematite, and the better the reducibility; the degree of low-temperature reduction disintegration is primarily determined by the open porosity and original hematite content of the lump ore at high temperatures; the lower the open porosity at high temperature and the higher the original hematite content, the greater the degree of reduction disintegration.

(3) The three lump ores' overall performances are appropriate for blast furnace ironmaking, but their reasonable ratios should be advised by optimizing the blast furnace burden structure to accomplish the objective of lower production costs and fewer carbon emissions.

Author Contributions: Conceptualization, D. Z. and Y.J.; methodology, Y.J.; software, Y.J.; validation, D.Z., Y.J. and J.P.; formal analysis, Y.J.; investigation, D.Z.; resources, D.Z.; data curation, C.Y.; writing—original draft preparation, Y.J..; writing—review and editing, D.Z..; visualization, D.Z..; supervision, J.P.; project administration, Y.J.; funding acquisition, Y.J.. All authors have read and agreed to the published version of the manuscript.

Funding: This research received no external funding.

Institutional Review Board Statement: Not applicable.

Informed Consent Statement: Not applicable.

Data Availability Statement: The study did not report any data.

Conflicts of Interest: The authors declare no conflict of interest.

References

1. Chakravarty, S.; Bhattacharyya, P.; Chatterjee, S.S.; Singh, B.N. Utilisation of Iron ore Fines in Alternative Iron making processes—An Indian perspective. *Nature* **2000**, *334*, 338–340.
2. An, X.; Wang, J.; Lan, R.; Han, Y.; Xue, Q. Softening and Melting Behavior of Mixed Burden for Oxygen Blast Furnace. *J. Iron Steel Res. Int.* **2013**, *20*, 11–16. https://doi.org/10.1016/S1006-706X(13)60090-4.
3. Li, Y.-F.; He, Z.-J.; Zhan, W.-L.; Kong, W.-G.; Han, P.; Zhang, J.-H.; Pang, Q.-H. Relationship and Mechanism Analysis of Soft-Melt Dropping Properties and Primary-Slag Formation Behaviors of the Mixed Burden in Increasing Lump Ore Ratio. *Metals* **2020**, *10*, 1254. https://doi.org/10.3390/met10091254.
4. Yu, Y.; Feng, G.; Su, D. Measures of decreasing blast furnace fuel consumption and improving sinter performance in guofeng. *J. Iron Steel Res. Int.* **2008**, *15*, 9–12. https://doi.org/10.1016/S1006-706X(08)60240-X.
5. Wu, S.; Liu, X.; Zhou, Q.; Xu, J.; Liu, C. Low Temperature Reduction Degradation Characteristics of Sinter, Pellet and Lump Ore. *J. Iron Steel Res. Int.* **2011**, *18*, 20–24. https://doi.org/10.1016/S1006-706X(11)60098-8.
6. Lu, W.-K. The search for an economical and environmentally friendly ironmaking process. *Met. Mater. Trans. B* **2001**, *32*, 757–762. https://doi.org/10.1007/s11663-001-0062-2.
7. Jie, L.; Hongyu, Z.; Mingshun, Z.; Liwei, Z.; Hui, Z.; Libing, X. Rational burden structure of blast furnace based on softening and melting property. *Gangtie* **2016**, *51*, 11–15.
8. Prakash, S. Nonisothermal kinetics of iron-ore reduction. *Ironmak. Steelmak.* **1994**, *21*, 237–243.
9. Wu, S.; Han, H.; Liu, X.; Wang, H.; Xue, F. Highly effective use of Australian Pilbara blend lump ore in a blast furnace. *Rev. Metall.* **2010**, *107*, 187–193. https://doi.org/10.1051/metal/2010021.
10. Ellis, B.G.; Loo, C.E.; Witchard, D. Effect of ore properties on sinter bed permeability and strength. *Ironmak. Steelmak.* **2007**, *34*, 99–108. https://doi.org/10.1179/174328107X165726.
11. Zhang, S.; Xue, X.; Liu, X.; Duan, P.; Yang, H.; Jiang, T.; Wang, D.; Liu, R. Current situation and comprehensive utilization of iron ore tailing resources. *J. Min. Sci.* **2006**, *42*, 403–408. https://doi.org/10.1007/s10913-006-0069-9.
12. Nagahiro, K.; Okazaki, T.; Nishino, M. Activities and technologies for environmental protection at Nippon Steel: A perspective. *Ironmak. Steelmak.* **2005**, *32*, 227–234. https://doi.org/10.1179/174328105X28856.
13. Li, X.; Zhang, J.; Su, B.; Yao, C.; Zhang, C. Performance evaluation of lump ores for blast furnace based on principle component analysis. *J. Cent. South Univ.* **2016**, *47*, 2943–2950.
14. Wang, X.; Zhang, J.; Liu, Z.; Liu, X.; Wang, R.; Zhenting, X.U. Influence of lump ore on metallurgical properties of blast furnace burden. *Res. Iron Steel.* **2017,** *45,* 1–5.
15. Wu, S.; Han, H.; Xu, H.; Wang, H.; Liu, X. Increasing Lump Ores Proportion in Blast Furnace Based on the High-temperature Interactivity of Iron Bearing Materials. *ISIJ Int.* **2010**, *50*, 686–694. https://doi.org/10.2355/isijinternational.50.686.
16. Wu, S.-L.; Xu, H.-F.; Tian, Y.-Q. Evaluation of lump ores for use in modern blast furnaces as part of mixed burden practice. *Ironmak. Steelmak.* **2009**, *36*, 19–23. https://doi.org/10.1179/174328107X167931.

17. Hongwei, G.; Guangqing, Y.; Jianliang, Z.; Jiugang, S.; Yuandi, F.; Dan, W. Effect of Mixed Charge of Ore and Lump Coal on the Softening-Melting Property of the Burden. In Proceedings of the 4th International Symposium on High-Temperature Metallurgical Processing, San Antonio, TX, USA, 3–7 March 2013.
18. Liu, X.; Honeyands, T.; O'Dea, D.; Li, G. *New Techniques to Measure Softening and Melting Properties of Mixed Burdens of Lump Ore and Sinter*; In 11st CSM Congress, Beijing. 2017.
19. Ta, H.T. MAC Lump Properties Study and Plant Performance at Baosteel Stainless Steel. In Proceedings of the 5th International Congress on the Science and Technology of Ironmaking, 19–23 October 2009, Shanghai, China.
20. Loo, C.E.; Matthews, L.T.; O'dea, D.P. Lump Ore and Sinter Behaviour during Softening and Melting. *ISIJ Int.* **2011**, *51*, 930–938. https://doi.org/10.2355/isijinternational.51.930.
21. Bristow, N.J.; Goss, J.; Waters, A.G. Influence of structural changes on the reducibility of iron ores. *Iron Steelmak.* **1992**, *13*, 83–92.
22. Harvey, T. *Influence of Mineralogy and Pore Structure on the Reducibility and Strength of Iron Ore Sinter;* Ph.D. Thesis, University of Newcastle, February, 2020.
23. Hoque, M.M.; Doostmohammadi, H.; Mitra, S.; O'dea, D.; Liu, X.; Honeyands, T. High Temperature Softening and Melting Interactions Between Newman Blend Lump and Sinter. *ISIJ Int.* **2021**, *61*, 2944-2952. https://doi.org/10.2355/isijinternational.ISIJINT-2021-198.